doi:10.1016/S0022-2836(02)01008-2 available online at http://www.idealibrary.com on IDEAL® J. Mol. Biol. (2002) 323, 739–750

JMB

Structural Effects of Cofilin on Longitudinal Contacts in F-actin

Andrey A. Bobkov[1]*, Andras Muhlrad[2], Kaveh Kokabi[1] Sergey Vorobiev[3], Steven C. Almo[3] and Emil Reisler[1]

[1]*Department of Chemistry and Biochemistry and the Molecular Biology Institute, University of California, Los Angeles, CA 90095, USA*

[2]*Department of Oral Biology School of Dental Medicine Hebrew University of Jerusalem P.O. Box 12272, Jerusalem 91120, Israel*

[3]*Department of Biochemistry Albert Einstein College of Medicine, New York, NY 10461 USA*

**Corresponding author*

Structural effects of yeast cofilin on skeletal muscle and yeast actin were examined in solution. Cofilin binding to native actin was non-cooperative and saturated at a 1:1 molar ratio, with $K_d \leq 0.05$ μM for both CaATP–G-actin and F-actin. Cofilin binding enhanced the fluorescence of dansyl ethylenediamine (DED) attached to Gln41 on the DNase I binding loop of skeletal muscle F-actin and decreased the fluorescence of AEDANS at Cys41 on yeast Q41C/C374S mutant F-actin. However, cofilin had no effect on the spectral properties of DED or AEDANS on CaATP–G-actin. Fluorescence energy transfer (FRET) from tryptophan residues to DED at Gln41 on skeletal muscle actin and to AEDANS at Cys41 on yeast Q41C/C374S actin was decreased by cofilin binding to F- but not to G-actin. Cofilin inhibited strongly the rate of interprotomer disulfide cross-linking of Cys41 to Cys374 on yeast Q41C mutant F-actin. Binding of cofilin enhanced excimer formation between pyrene probes attached to Cys41 and Cys374 on Q41C F-actin. These results indicate that cofilin alters the interface between subdomains 1 and 2 and shifts the DNase I binding loop away from subdomain 1 of an adjacent actin protomer. Cofilin reduced FRET from tryptophan residues to 4-azido-2-nitrophenyl-putrescine (ANP) at Gln41 in skeletal muscle F-but not in G-actin. However, following the interprotomer cross-linking of Gln41 to Cys374 in F-actin by ANP, cofilin binding did not change FRET from the tryptophan residues to ANP. This suggests that cofilin binding and the conformational effect on F-actin are not coupled tightly. Overall, this study provides solution evidence for the weakening of longitudinal, subdomain 2/1 contacts in F-actin by cofilin.

Keywords: actin; ADF; cofilin; DNase I binding loop; longitudinal contacts

Introduction

There are several known families of actin-binding proteins, which branch, cross-link, sever, cap, stabilize, depolymerize, nucleate and otherwise regulate the actin dynamics in cells. Small, monomeric proteins that belong to the actin-depolymerizing factor (ADF)/cofilin family play a central role in the regulation of actin dynamics in cells. They are required for cell motility, viability and development of embryonic tissues.[1–4] The nomenclature of the ADF/cofilin (AC) family is rather complicated, as AC proteins from different sources have been named depactin, destrin, actophorin, ADF, and cofilin.[4] Despite their low average level of sequence identity (~40%), AC proteins from different species have remarkably similar 3D structures.[5] Because of their structural and functional similarities, AC proteins, and ADF and cofilin in particular, are increasingly treated as isoforms in the recent literature.

It is established that AC promotes F-actin dynamics and cell motility by accelerating actin turnover; however, the particular mechanism of its cellular function is still disputed. Some authors emphasize actin-severing and depolymerizing

Present address: A. A. Bobkov, The Burnham Institute, 10901 North Torrey Pines Road, La Jolla, CA 92037, USA.

Abbreviations used: AC, ADF/cofilin; ADF, actin-depolymerizing factor; ANP, 4-azido-2-nitrophenyl-putrescine; DED, dansyl ethylenediamine; FRET, fluorescence resonance energy transfer; IAEDANS, 5-[[((2-iodoacetyl)amino)ethyl]amino]naphthalene-1-sulfonic acid.

E-mail address of the corresponding author: abobkov@burnham.org

properties of AC,[6–8] while others have played down the actin-severing function of AC and attribute its effect to the simultaneous acceleration of monomer dissociation from the pointed ends and association at the barbed ends of F-actin.[9,10] A combination of both mechanisms was suggested as well to explain AC action on F-actin.[11,12]

Structural effects of AC proteins on F-actin have been examined by electron microscopy (EM) and an initial report indicated that AC binding resulted in a significant change in the twist of actin filaments.[13] Later, it was suggested that ADF does not actively change twist, but preferentially stabilizes one of the existing twist variations in F-actin thereby shifting the equilibrium between the "normal" and "ADF-twist" conformations towards the latter.[9,14] These results led to the conclusion that AC binding weakens longitudinal contacts in F-actin. Furthermore, the crystal structures of G-actin and AC were fit into the EM reconstruction of the F-actin–AC complexes to provide models of cofilin[13] and ADF[14] bound to F-actin. In these models, AC is bound to two adjacent protomers in F-actin, and overlaps subdomains 1 and 2 and the interprotomer interface between them.

The number of publications focused on kinetic studies of the interactions of AC proteins with actin and EM reconstruction of their complexes is increasing steadily. However, there is an evident lack of studies that would bridge these two directions and examine the structural effects of AC on F-actin in solution. We describe the first in a series of studies designed to fill this gap. Our approach here is to position fluorescent probes in the dynamic structural elements involved in the intermolecular contacts in F-actin. Cofilin effects on actin conformation in the vicinity of the probes can be monitored *via* changes in the spectral properties of these probes. This study is focused on the cofilin effects on the longitudinal subdomain 2/1 contacts in F-actin, which involve the DNase I binding loop (residues 38–52) and the C-terminal region on adjacent protomers.

It is easy to rationalize the targeting of the DNase I binding loop for monitoring the structural effects of cofilin on F-actin. In the Holmes[15] and Lorenz[16] models of F-actin structure, this loop was postulated to participate in the intermolecular longitudinal contacts. Owen & DeRosier[17] proposed that the DNase I binding loop, the C terminus, and hydrophobic plug interact cooperatively to form an intermolecular interface in F-actin. A number of other observations revealed an important role of this loop in the stabilization of F-actin structure and suggested that it can adopt different conformational states.[18–22] There have been several reports regarding dynamic properties of this loop[23] and its structural coupling with the C-terminal region of actin.[24,25] Finally, it was proposed that AC interacts directly with the DNase I binding loop in the complex with F-actin.[13,14]

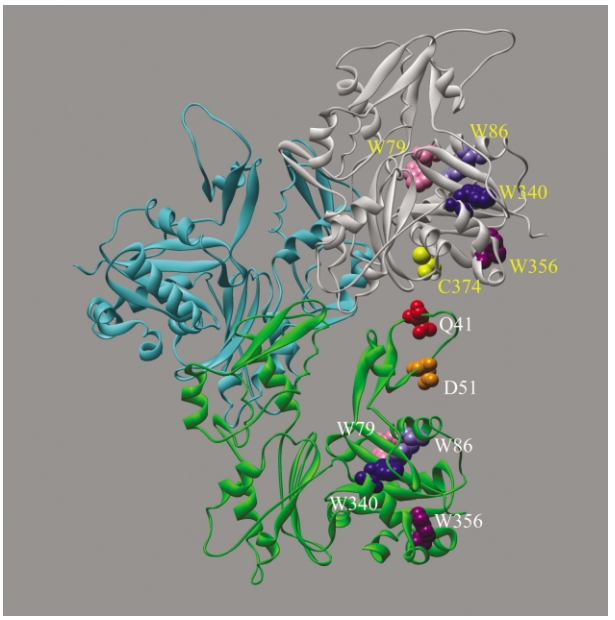

Figure 1. Three protomers in the molecular model of F-actin.[15] Protomers I (gray) and III (green) form longitudinal contacts in this representation. Tryptophan residues 79, 86, 340, and 356 are highlighted in these protomers. Residues 374 (C terminus, protomer I), 41 and 51 (DNase I binding loop, protomer III), which were used for attachment of fluorescent probes, are also highlighted.

Most previous studies on AC proteins were performed using rabbit skeletal muscle α-actin, since it can be obtained easily and in large quantities; however, the importance of using of AC and actin from the same organism has been emphasized[4] repeatedly.[8] One of the concerns is that a particular AC protein maybe "fine-tuned" to the actin from the same cellular system. To address this issue, we have studied the effects of yeast cofilin on both, rabbit skeletal muscle and yeast actins. In the rabbit skeletal muscle α-actin, probes were attached to Gln41 in the DNase I binding loop (Figure 1). We have used yeast actin mutants Q41C/C374S and D51C/C374S (in which Gln41 and Asp51 were substituted with cysteine residues) to introduce fluorescent probes to the DNase I binding loop (Figure 1). To probe the interface between the DNase I binding loop and C terminus in F-actin we have: (i) cross-linked Gln41 to Cys374 in the skeletal muscle α-actin; (ii) cross-linked Cys41 to Cys374 in the Q41C yeast actin mutant; and (iii) formed a pyrene excimer between two labels attached to Cys41 and Cys374 in the yeast actin mutant.

Results

Cofilin binding to actin

Cofilin binding to unlabeled wild-type (WT) yeast and skeletal muscle α-actin was monitored

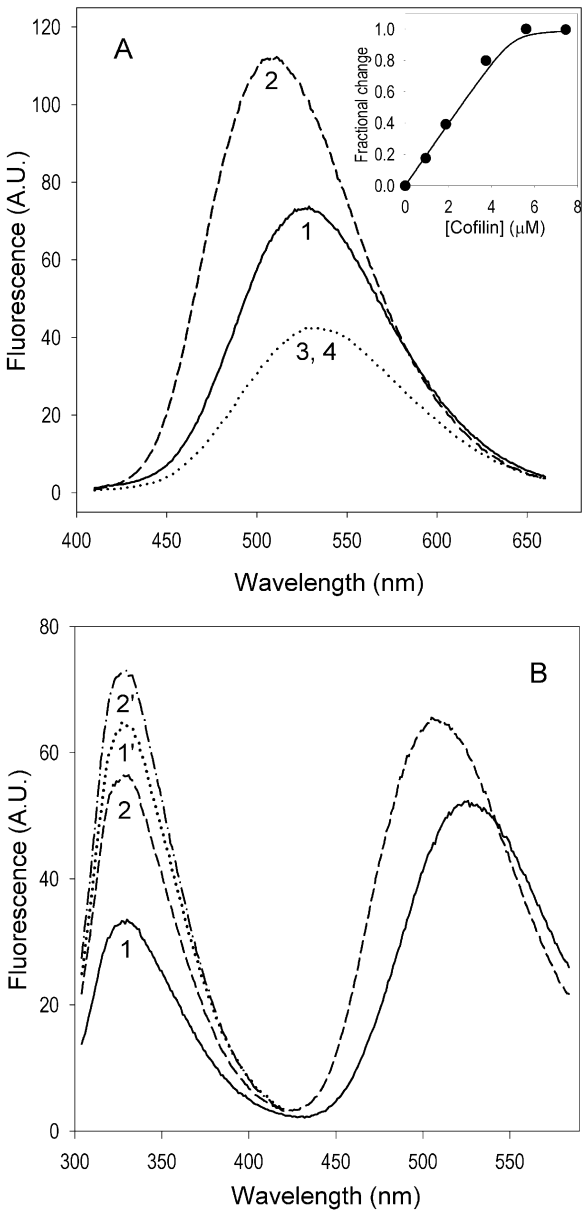

Figure 2. Fluorescence emission spectra of DED at Gln41 in skeletal muscle α-actin. (a) Emission spectra for DED excited directly at $\lambda = 334$ nm were collected for DED–F-actin (1) in the absence and (2) in the presence of 7.4 μM cofilin, and for DED–G-actin (3) in the absence and (4) in the presence of 7.4 μM cofilin. Spectra 3 and 4 are superimposed. Inset: titration of DED–F-actin with cofilin was monitored *via* an increase in the DED emission at $\lambda_{max} = 506$ nm. The calculated curve (equation (2)) describes equimolar binding of cofilin to actin with $K_d = 0.05$ μM. (b) Emission spectra of DED–F-actin using $\lambda_{ex} = 295$. Spectra (1) and (2) are for the same solutions as in (a). Spectra (1′) and (2′) correspond to the unlabeled F-actin in the absence and presence of 7.4 μM cofilin, respectively. The concentration of actin was 5.0 μM in all cases.

via tryptophan intrinsic fluorescence, at $\lambda = 320$ nm, which increases upon cofilin binding to both polymeric (Figure 2(b), spectra 1′ and 2′) and monomeric (data not shown) forms of actin. Stoichiometric binding of cofilin to F and G-actin results in ~11% and ~7% net increase in their tryptophan fluorescence, respectively. We have also measured the binding of cofilin to F-actin *via* light-scattering (as shown in Figure 6(b)). These measurements demonstrated tight binding of cofilin to WT yeast and skeletal muscle α-actin, with an equilibrium dissociation constant (K_d) ≤ 0.05 μM for both G-actin and F-actin. Similar K_d values were reported for the binding of ADF from *Arabidopsis thaliana* to rabbit skeletal muscle G-actin.[9] In analogy with ADF,[9] cofilin binding to F-actin was non-cooperative and saturated at a 1:1 molar ratio to actin.

Tryptophan fluorescence and light-scattering were used to assess cofilin affinity to the labeled actins listed in Table 1. Unless stated otherwise, the labeling did not affect the binding of cofilin to actin significantly.

We have estimated the depolymerization of yeast and rabbit skeletal muscle F-actin by cofilin in ultracentrifugation pelleting experiments. Solutions of F-actin, with and without cofilin, were pelleted in the airfuge and the amount of depolymerized actin in the supernatant was assessed from the intensity of Coomasie-stained actin bands following SDS-PAGE. Under conditions of our spectroscopic and cross-linking experiments (10 mM Tes (pH 7.5), 0.2 mM $CaCl_2$, 3.0 mM $MgCl_2$, 0.2 mM ATP, 1.0 mM DTT, 4.0–10 μM actin, 0.95–13 μM cofilin) the extent of actin depolymerization was consistent with the results of prior studies that reported steady-state concentrations of 0.7 μM and 0.6 μM for rabbit skeletal muscle[9] and yeast actin,[26,27] respectively, depolymerized by yeast cofilin. Steady-state light-scattering measurements on the labeled F-actin did not detect significant depolymerization of actin, probably because of the concomitant signal increase due to cofilin binding to F-actin and polymer stabilization by the incorporated labels.[28] On the other hand, stopped-flow light-scattering measurements (see Figure 6(b)) differentiated well between the fast cofilin binding and the much slower and limited depolymerization process.

Effects of cofilin on Gln41 DED-labeled skeletal muscle α-actin

It has been shown before that Gln41 on skeletal muscle α-actin can be labeled specifically with dansyl cadaverine[29] or dansyl ethylenediamine (DED)[28] and that these fluorescent labels are sensitive to the environment of the DNase I binding loop and actin polymerization. We have taken advantage of these observations to study the effects of cofilin binding on the DNase I binding loop conformation. Spectrum 3 in Figure 2(a) shows the fluorescence emission of DED-labeled skeletal muscle G-actin, with λ_{max} at 532 nm. As observed before,[28] actin polymerization caused an increase in the intensity and a slight blue shift (to $\lambda_{max} = 529$ nm) of the DED spectrum (Figure 2(a),

Table 1. Actins and probes used in the study

Actin	Residue labeled	Probe	Location on actin
Skeletal muscle α-actin	Q41	DED, ANP	DNase I binding loop
	Q41 and C374	ANP-cross-link	DNase I binding loop/C terminus
Yeast actin mutants			
Q41C/C374S	C41	IAEDANS	DNase I binding loop
D51C/C374S	C51	IAEDANS	DNase I binding loop
Q41C	C41 and C374	Pyrene maleimide, S–S cross-link	DNase I binding loop/C terminus

spectrum 1). Cofilin binding caused further increase in the intensity and an additional blue shift (to $\lambda_{max} = 506$ nm) of the emission spectrum of DED on F-actin (Figure 2(a), spectrum 2), but had no effect on the spectral properties of DED on G-actin (Figure 2(a), spectrum 4). This indicates that cofilin binding changes the environment of DED on the DNase I binding loop in F-actin, but not in G-actin. A recent study by Dedova *et al.*[30] reported cofilin-induced changes in the fluorescence of a similar probe, albeit with a longer linker chain (dansyl cadaverine), attached to Gln41 on G-actin. Although these authors used an isoform of cofilin (from chick embryo) different from that employed by us (from yeast), it is likely that the local environment of the DNase binding loop in G-actin and its response to cofilin binding are sensitive to the type of probe attached to Gln41.

We have used DED fluorescence change at $\lambda = 506$ nm to estimate the K_d for the cofilin–DED–F-actin complex. Fitting the experimental data (Figure 2(a), inset) to equation (2) resulted in a K_d value ≤ 0.05 μM, indicating that the affinity of cofilin for F-actin is not decreased significantly by labeling the latter with DED.

To determine whether cofilin binding induces a movement of the DNase I binding loop, we examined fluorescence resonance energy transfer (FRET) from tryptophan to DED at Gln41 in skeletal muscle α-actin. The fluorescence spectrum of DED-labeled F-actin excited at 295 nm (Figure 2(b)) consists of the tryptophan (donor, $\lambda_{max} = 330$ nm) and DED (acceptor, $\lambda_{max} = 529$ nm) emission peaks. A comparison of the emission spectra of labeled and unlabeled F-actin (Figure 2(b), spectra 1 and 1′, respectively) shows a substantial decrease in the intensity of donor fluorescence in the presence of the DED acceptor, indicative of FRET from tryptophan to DED at Gln41. The efficiency of this process, corrected for the extent of actin labeling by DED (88(±3)%), is ~64% in F-actin and only 19% in G-actin (Table 2), revealing a major contribution of interprotomer FRET to the high transfer efficiency in F-actin. Cofilin binding to F-actin increased both the tryptophan and DED fluorescence (Figure 2(b), spectrum 2). Strikingly, the cofilin-associated increase in DED emission of the labeled F-actin is smaller by 25(±5)% after excitation at 295 nm (Figure 2(b), spectra 1 and 2) than when excited at 334 nm (Figure 2(a) spectra 1 and 2). This result implies a decrease in FRET from tryptophan to DED, which is confirmed by examining the donor fluorescence; namely, the tryptophan fluorescence recovery in the labeled F-actin due to cofilin binding (Figure 2(b), spectra 1 and 2). Correcting for the cofilin-induced changes in tryptophan fluorescence of unlabeled actin (Figure 2(b), spectra 1′ and 2′), there is ~33% loss of FRET (from 64% to 31%, Table 2) from tryptophan to DED.

Actin has four tryptophan residues, 79, 86, 340, and 356, all of them located in subdomain 1 (Figure 1). In principle, these tryptophan residues, from both protomer I (green) and protomer III (gray) in F-actin (Figure 1), can act as FRET donors to DED located at Gln41 (on protomer I). As shown recently,[31] the intrinsic fluorescence of yeast actin is dominated by Trp340 and Trp356, which account for ~37% and 51% of the total quantum yield of actin, respectively. Theoretical analysis of the microenvironment of rabbit skeletal muscle α-actin tryptophans led to the same conclusions.[32] According to these findings, we can calculate[33] on the basis of the Holmes[15] model of actin filament, and $R_0 = 21$ Å for the tryptophan–dansyl (donor–acceptor) pair,[34] the overall FRET from tryptophan to DED on Gln41. The bulk of such FRET is interpreted to come from Trp340 and Trp356 on the adjacent protomer (III) in F-actin. Since interprotomer energy transfer is the major component of FRET in DED–F-actin, the loss of FRET can be interpreted to be a consequence of cofilin-induced movement of the DNase I binding loop of protomer I away from subdomain I of protomer III

Table 2. Efficiencies of FRET from tryptophan residues to ANP or DED on Q41 in skeletal muscle α-actin

	FRET efficiency (%)		
Actins	Without cofilin	With cofilin	Δ
ANP-labeled G-actin	21	20	1
ANP-labeled F-actin	74	47	27
ANP–cross-linked F-actin	62	64	2
DED-labeled G-actin	19	15	4
DED-labeled F-actin	64	30 (31)[a]	33

All experiments were repeated on at least three different preparations of the labeled actins. Experimental errors for the data do not exceed 5%. ANP-labeled and DED-labeled actins were used at concentrations of 4.0 μM and 5.0 μM, respectively. Cofilin was added to these actins at 4.0 μM and 7.4 μM, respectively.

[a] FRET efficiency shown in parentheses is the value corrected for depolymerization of F-actin by cofilin (10%).

(Figure 1). Notably, cofilin has only a small effect on FRET in DED–G-actin (Table 2). This indicates that cofilin induces movement of the DNase I binding loop in F-actin and much less in G-actin. A possible movement of this loop in G-actin by cofilin was implied by the reported small change in the distance between fluorescent probes on Gln41 and Cys374 on G-actin at pH 8.0 (~1.4 Å) and a larger change at pH 6.8.[30] However, because the C-terminal acceptor site (Cys374) is known to be mobile and the probes attached there are influenced strongly by cofilin,[30] the FRET results of these authors do not prove the movement of the DNase binding loop in G-actin.

Cofilin interaction with AEDANS-labeled Q41C/C374S yeast actin

To confirm the effect of cofilin on the DNase I binding loop with a homologous actin (i.e. in a yeast actin–cofilin system), we used Q41C/C374S yeast actin mutant[35] in which Cys41 was labeled with AEDANS. Cofilin binding to AEDANS–F-actin caused a 9(±5)% decrease in AEDANS fluorescence when using $\lambda_{ex} = 334$ nm (data not shown). The decrease associated with cofilin binding was substantially larger (40(±10)%) when AEDANS–F-actin was excited at 295 nm, i.e. through tryptophan residues. This shows that, in analogy to its effect on Gln41 DED-labeled α-actin, cofilin reduces energy transfer from tryptophan to AEDANS at Cys41 in yeast F-actin. Thus, in yeast actin, as in skeletal muscle α-actin, cofilin displaces the DNase I binding loop away from the subdomain 1 of the upper protomer in F-actin (Figure 1). Similar to the effect of cofilin on DED fluorescence of α-actin, the change induced in AEDANS fluorescence (with $\lambda_{ex} = 295$ nm) was non-cooperative and yielded a K_d value ≤0.05 μM. Thus, Cys41 labeling with IAEDANS does not decrease the binding of cofilin to Q41C/C374S actin significantly.

Monitoring the interprotomer interface in F-actin *via* the Cys41–Cys374 interrelationship

The changes in the interprotomer subdomain 2/1 interface in Q41C F-actin[35] due to cofilin binding were monitored by assaying the proximity of Cys41 and Cys374 on the adjacent actins in excimer fluorescence and disulfide cross-linking experiments. Fluorescence emission spectrum of Cys41 and Cys374 pyrene-labeled Q41C G-actin is shown in Figure 3, spectrum 3. Upon polymerization, the pyrene label at Cys41 stacks with the label at Cys374 of the next protomer in the strand, producing an excimer emission band with λ_{max} at 476 nm (Figure 3, spectrum 1).[36] Cofilin binding to the pyrene–F-actin enhanced excimer formation, as detected by an increase in the intensity of the excimer band and a simultaneous decrease in the intensity of the pyrene monomer band, between 370 nm and 405 nm (Figure 3, spectrum 2). The

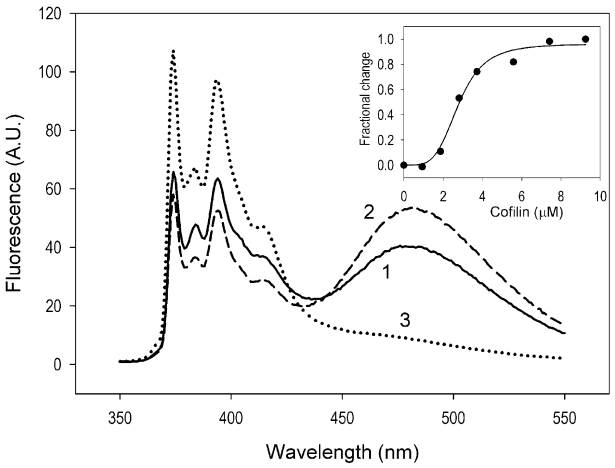

Figure 3. Fluorescence emission spectra of pyrene-labeled Q41C yeast actin. Spectra were collected for pyrene–F-actin (1) in the absence and (2) in the presence of 7.5 μM cofilin, and (3) for pyrene–G-actin. The concentration of actin was 5.0 μM. Inset: a titration of pyrene–F-actin with cofilin observed through an increase in pyrene excimer fluorescence at λ = 480 nm. The excitation wavelength was set at 344 nm. Excimer fluorescence changes were fit to equation (3) to yield $n = 4.2$ and $K_{0.5} = 2.7$ μM.

most likely explanation of this effect is that cofilin binding promotes a structural rearrangement of longitudinal contacts in F-actin, thereby moving the probes on residues 41 and 374 to positions more favorable for excimer formation. Notably, the effect of cofilin binding on excimer formation exhibited positive cooperativity (Figure 3, inset). This may be due to a stabilization of longitudinal contacts in F-actin by pyrene stacking and a possible inhibition of binding and/or conformational effect of cofilin on the double-labeled F-actin at low molar ratios of cofilin to actin.

More direct and quantitative evidence for cofilin-induced changes in Cys41–Cys374 separation on adjacent protomers in F-actin was obtained by determining the rates of spontaneous disulfide cross-linking of Q41C F-actin in the presence and in the absence of cofilin. The cross-linking reaction was monitored *via* SDS-PAGE by measuring the rate of disappearance of the monomer actin band due to F-actin cross-linking. The gel patterns of the disulfide cross-linking reactions in the presence and in the absence of cofilin are very different (Figure 4(a)), showing large rate differences between the two reactions (Figure 4(b)). The first-order rate constants for disulfide cross-linking of Cys41 to Cys374 were about 20-fold smaller in the presence than in the absence of cofilin (Figure 4(b)). Similar inhibition of disulfide cross-linking in Q41C F-actin by cofilin was observed on a much shorter time-scale (~20 minutes) using copper-catalyzed oxidation reactions (data not shown). The strong inhibition of disulfide formation by cofilin reveals that the mean distance

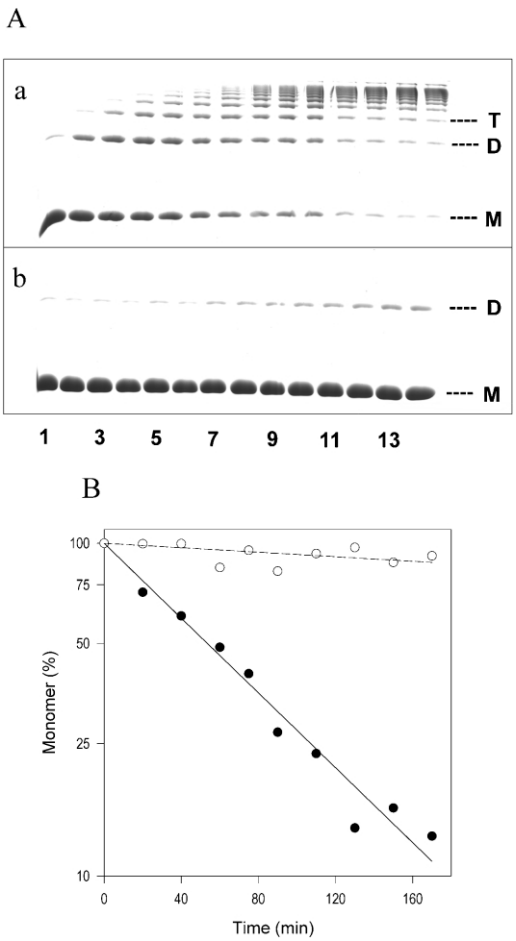

Figure 4. Disulfide cross-linking of Q41C F-actin. (a) SDS-PAGE patterns of F-actin (10 μM) cross-linked in the absence (a) and in the presence (b) of cofilin (10 μM). Lanes from 1 to 14 are for reaction aliquots taken after 0, 20, 40, 60, 75, 90, 110, 130, 150, 170, 190, 210, 230, and 250 minutes of the cross-linking reaction, respectively. Symbols m, d and t correspond to actin monomer, dimer and trimer disulfide-bonded species. Reaction conditions were as described in Materials and Methods. (b) Semilogarithmic plots of monomer actin band disappearance on SDS-PAGE with time of the reaction. The data were taken from (a)a for the reaction in the absence of cofilin (●) and from (a)b for the reaction in the presence of cofilin (○). The first order rate constants for disulfide cross-linking of Q41C F-actin, as determined from the linear semilogarithmic plots, were $5.6(\pm 0.2) \times 10^{-3}\,\mathrm{min}^{-1}$ and $0.39(\pm 0.1) \times 10^{-3}\,\mathrm{min}^{-1}$ in the absence and in the presence of cofilin, respectively.

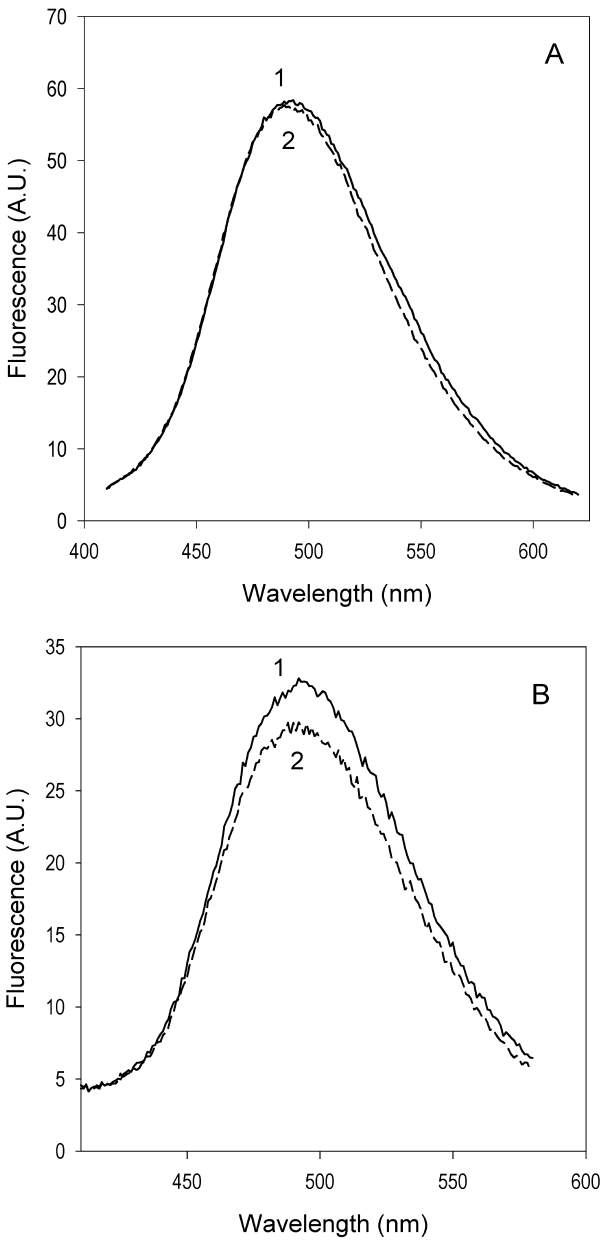

Figure 5. Fluorescence emission spectra of AEDANS at Cys51 in D51C/C374S yeast actin. AEDANS was excited either (a) directly at λ = 338 nm, or (b) *via* tryptophan at λ = 295 nm. Spectra are shown for 5.0 μM AEDANS–F-actin (1) in the absence and (2) in the presence of 6.5 μM cofilin.

between Cys41 and Cys374 on adjacent actin protomers in F-actin is increased by cofilin.

Cofilin binding to AEDANS-labeled D51C/C374S yeast actin

To gain further insight into cofilin-induced movement of the DNase I binding loop in F-actin, we employed another cysteine mutant of yeast actin, D51C/C374S.[37] This mutant allowed AEDANS labeling of Cys51 in the DNase I binding loop, at its C-terminal site, near the base of the loop (Figure 1). Cofilin-induced changes in the fluorescence of AEDANS at residue 51 in F-actin (Figure 5) did not exceed 10% (when excited at 295 nm, Figure 5(b)) and were substantially smaller than those for DED (or AEDANS) located at residue 41 (Figure 2), which is at the top of the loop. These observations indicate that cofilin induces a larger motion at the top than at the base of the DNase I binding loop in F-actin, resulting in a swing-like movement of this loop away from the C terminus of the upper protomer (III) in F-actin (Figure 1).

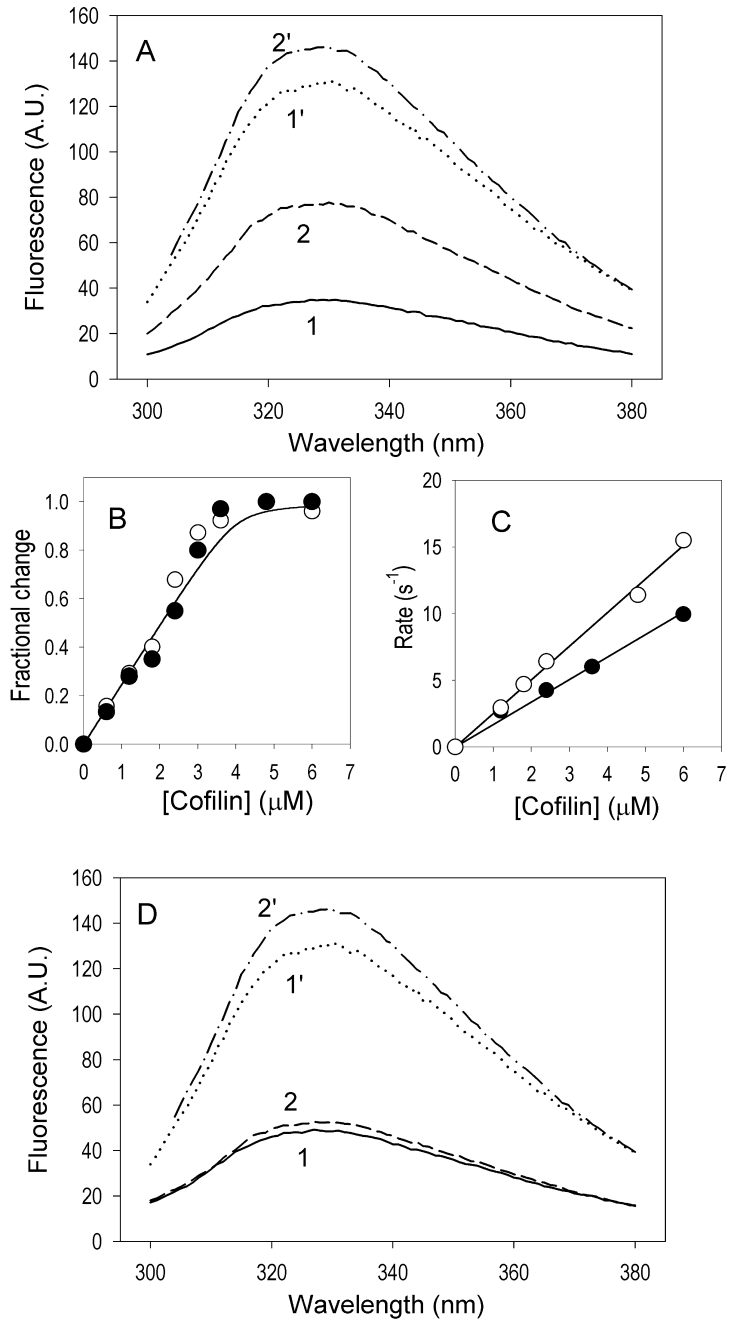

Figure 6. Tryptophan fluorescence emission spectra of ANP-labeled and ANP–cross-linked skeletal muscle F-actin. (a) ANP–F-actin (1) in the absence and (2) in the presence of 4.0 μM cofilin, and unlabeled F-actin (1′) in the absence and (2′) presence of 4.0 μM cofilin. (b) The binding of cofilin to ANP–F-actin was followed *via* increases in light-scattering (open circles) and tryptophan fluorescence (filled circles) signals. Both signals were obtained from stopped-flow measurements described in Materials and Methods. (c) Rates of light-scattering (open circles) and tryptophan fluorescence (filled circles) increase upon cofilin binding to actin. The rates were obtained by fitting stopped-flow traces to a single-exponential equation. (d) ANP–cross-linked-F-actin (1) in the absence and (2) in the presence of 4.0 μM cofilin, and unlabeled F-actin (1′) in the absence and (2′) in the presence of 4.0 μM cofilin. The concentration of actin was 4.0 μM in all experiments.

Cofilin effects on ANP-labeled and ANP-cross-linked skeletal muscle α-actin

If the interpretation of the above results in terms of cofilin-induced movement of the DNase I binding loop in F-actin is correct, then the cross-linking of this loop to the C terminus of the upper protomer should reduce or abolish the cofilin effect. To test this, we took advantage of a hetero-functional photo-cross-linking reagent, 4-azido-2-nitrophenyl-putrescine (ANP), which was shown before to cross-link Gln41 to Cys374 on the adjacent protomer within the same strand of the long-pitch helix.[38] ANP quenches actin tryptophan fluorescence efficiently (Figure 6(a), spectra 1 and 1′), serving as a non-fluorescent FRET acceptor for these donors. FRET efficiency is much higher in F-actin than in G-actin (Table 2), indicating that, as in DED–F-actin, the interprotomer energy transfer is the major component of FRET in ANP-labeled F-actin. Similar to DED–F-actin (Figure 2, Table 2), the binding of cofilin to ANP–F-actin caused a substantial increase in tryptophan fluorescence, indicating ~27% decrease in the efficiency of FRET from tryptophan to ANP (Figure 6(a), spectrum 2; Table 2).

Cofilin-induced changes in tryptophan fluorescence followed closely the binding of cofilin to actin, as measured from fluorescence and light-scattering amplitude changes in stopped-flow

experiments (Figure 6(b)). Such light-scattering measurements readily distinguish between the fast-amplitude increase due to cofilin binding to F-actin and the slower, marginal for ANP–F-actin, decrease in light-scattering due to actin depolymerization, thereby simplifying the binding measurements. Fitting of these data to the binding equation (equation (2)) yielded the same K_d value (≤ 0.05 μM) as that reported above for other actin preparations. It may be noted, however, that the precision of our measurements is insufficient to preclude the fitting of these data with a curve showing a low-level cooperativity of cofilin binding and fluorescence changes in F-actin. The observed rates of fluorescence change (Figure 6(c)) were about 50% slower than the rates of light-scattering increase (with the respective second-order rate constants of 1.6 $\mu M^{-1} s^{-1}$ and 2.5 $\mu M^{-1} s^{-1}$), revealing that the conformational change in F-actin is slower than its binding of cofilin. Binding of cofilin to ANP–G-actin had virtually no effect on FRET efficiency (Table 2). Thus, cofilin effects on ANP-labeled actin were very similar to those for DED-labeled actin and confirmed again, with a different acceptor on Gln41, that cofilin binding induces movement of the DNase I binding loop in F-actin, and little, if any, movement in G-actin.

Cross-linking of ANP-labeled F-actin resulted in formation of a bond between Gln41 and Cys374 on protomers I and III, respectively[38] (green and white protomers in Figure 1). Similar to the ANP-labeled F-actin (Figure 6(a), spectrum 1), the ANP–cross-linked F-actin (Figure 6(d), spectrum 1) had a strongly reduced tryptophan fluorescence due to energy transfer between tryptophan residues and the ANP (Table 2). However, in contrast to the ANP-labeled F-actin (Figure 6(a) spectrum 2, and Table 2), cofilin had virtually no effect on FRET between tryptophan residues and ANP in the ANP–cross-linked actin (Figure 6(d), spectrum 2). Importantly, light-scattering measurements showed that cofilin was able to bind well to the ANP–cross-linked F-actin (data not shown). Thus, as predicted above, this cross-linking prevents cofilin-induced movement of the DNase I binding loop, but not the binding of cofilin to F-actin.

Discussion

The pH-dependent depolymerization of actin by cofilin has been proposed to involve two mechanisms: the severing of filaments and the acceleration of their depolymerization at the pointed ends.[4,7,9,39] There is considerable interest in clarifying these processes at a molecular level. A potential explanation of cofilin action has been advanced on the basis of EM studies of F-actin–cofilin complexes. Several such studies have shown that the binding of cofilin induces or stabilizes filament conformations with a large twist change and much shorter cross-over length.[13,14,40] Although such conformations exist at low frequency in F-actin alone, the change in the mean twist weakens longitudinal and lateral contacts among adjacent protomers, leading, perhaps, to structural strain and severing of the filaments.

According to EM results, the changes in F-actin structure induced by cofilin involve a substantial tilt of actin subunits[13,14] and remodeling of interprotomer contacts. Cofilin appears to disrupt longitudinal contacts between subdomains 2 and 1, and subdomains 3 and 4. At the same time, according to a recent model,[41] the tilting of actin subunits by cofilin brings subdomain 2 of one protomer into closer contact with subdomain 3 of the protomer above it. The main goal of the present study was to evaluate, using cross-linking and fluorescence probes, the effect of cofilin binding on the longitudinal interprotomer subdomain 2/1 interface in F-actin under equilibrium solution conditions. The use of both rabbit skeletal muscle and yeast actin in this study is justified by their similar binding affinities to yeast cofilin, both in the presence and in the absence of probes attached to the DNase I binding loop. With only a single exception (two pyrene maleimide molecules attached to Cys41 and Cys374 in Q41C yeast actin), the binding titrations of actin by cofilin did not show the significant cooperativity observed in some prior studies.[10,13,39] Those studies used heterologous actin–AC pairs, which might account for the discrepancy.

The most striking effect of cofilin on subdomain 2/1 interface is the inhibition of disulfide bond formation between Cys41 and Cys374 in Q41C yeast F-actin. The presence of a small fraction of depolymerized actin in these experiments (monitored throughout the course of the reaction) cannot account for the large inhibition of the cross-linking. Importantly, as shown previously,[42] the disulfide cross-linking of this actin introduces only minimal perturbations in the filament structure and the reaction follows a random cross-linking mechanism. Thus, it appears that the inhibition of cross-linking by cofilin may be caused by shifts in the position/orientation of either the DNase I binding loop or the C terminus, by both of these, or even by steric hindrance due to cofilin binding to this region.[13] Our result is consistent with the proposed shift of subdomain 2 from its contacts with subdomain 1 above it, towards subdomain 3 of an adjacent protomer.[41]

The increase in excimer fluorescence of pyrene-labeled Q41C F-actin upon cofilin binding may appear counterintuitive, considering the inhibition of disulfide cross-linking by cofilin. However, it is difficult to translate changes in excimer fluorescence to changes in distance between Cys41 and Cys374 on adjacent protomers, especially in view of the uncertainty regarding the atomic position of the labeled Cys374. Because of the reagent size, the excimer stacking of pyrene maleimide probes can occur at thiol separations between 3 Å and 18 Å,[43] and depends on such factors as the

orientation of thiol groups, flexibility of attachments, and perhaps even the interaction of the pyrene moiety with a local hydrophobic environment. Thus, within the above range of thiol distances, the probability of excimer formation may even increase with the increase in their separation if the other factors promote probe stacking. Nevertheless, the distance between Cys374 and Gln41 in the model of the cofilin-tilted F-actin (~18 Å)[41] may be too large to reconcile with the increase in the excimer fluorescence by cofilin observed in this study.

Unambiguous evidence for the displacement of the DNase I binding loop from its mean position in F-actin by cofilin is provided by the large decrease in FRET from tryptophan to probes attached to residue 41 on actin. As argued in Results, the bulk of FRET between tryptophan donors and DED on Gln41 is intermolecular, involving Trp340 and Trp356 on one protomer and DED on the protomer below it. Using distances derived from the Holmes model of F-actin structure,[15] the quantum yields of actin tryptophan residues[31] and $R_0 = 21$ Å,[34] the calculated overall efficiency of FRET from all adjacent tryptophan residues to DED on Gln41 is $E = 54.8\%$. This is close to our measured value of $E = 64\%$ (Table 2), since a minor adjustment to the Holmes model (decreasing the distances from Gln41 to Trp340 and Trp356 by 1.5 Å) would yield a calculated $E = 63.4\%$. A consideration of slightly decreased separation of Gln41 from the next protomer tryptophan residues is justified by the disulfide cross-linking results (Figure 4(a)),[35] which indicate that the Holmes model of F-actin structure overestimates the interprotomer distance between Gln41 and Cys374. Notably, according to the above calculations, interprotomer FRET from Trp340 and Trp356 to DED on Gln41 accounts for ~87% of the overall FRET.

The interpretation of the cofilin-induced decrease in the above FRET (to ~31%, Table 2) can be simplified by a few approximations. These include: (i) neglecting changes in FRET from tryptophan residues other than Trp340 and Trp356 on the protomer above the labeled actin; (ii) allowing for an adjustment (~10%) in FRET due to DED–actin depolymerization (on the basis of different FRET efficiencies in G and F-actin, Table 2); and (iii) assuming equal displacement of residue 41 from the above two tryptophan residues. Using these simplifying approximations, Gln41 appears to be displaced by ~6 Å from Trp340 and Trp356. Such a displacement is consistent with the subunit tilt documented for cofilin-decorated skeletal muscle and yeast actin and with the shift in mass distribution associated with this tilt.[14] Our FRET results agree with the more detailed and refined model of actin decorated by cofilin in which more extensive filament tilt and domain rotations are proposed.[41] FRET efficiency $E = 35.0\%$ calculated for such a tilted actin trimer model is close to the experimentally determined $E = 31\%$ (Table 2). The difference between these two values corresponds to an additional displacement by 0.7 Å of Gln41 away from Trp340 and Trp356 (in the next protomer) compared to their distances in the tilted trimer model (24.7 Å and 22.2 Å, respectively). However, it must be emphasized that the assumptions used in the analysis of our FRET data (as listed above) preclude independent conclusions about the direction of the estimated Gln41 displacement. Irrespective of these details, the above FRET results strengthen the interpretation of the cofilin-induced inhibition of disulfide cross-linking in Q41C F-actin in terms of mass shifts that include the displacement of the DNase I binding loop away from the C terminus.

A cofilin-induced change in the DNase I binding loop can be deduced from the spectral changes of probes attached to residue 41. A blue shift in the emission spectrum of DED (on Gln41) F-actin and a significant increase in its fluorescence (Figure 2) suggest that the probe moves to a more hydrophobic environment. In the context of previous EM observations and our disulfide cross-linking and FRET results, the above change in DED fluorescence may be attributed to a shift of the probe site to new contact sites on adjacent protomers[39] or the interface with cofilin.[13] The latter possibility is suggested by the observation that longitudinal actin–cofilin–actin contacts are stronger than those of actin–actin. It may be possible to differentiate between these scenarios by appropriate cross-linking experiments, in which the site(s) (either on actin or on cofilin) cross-linked to the DNase I binding loop would be mapped and sequenced.

In addition to confirming the interprotomer FRET from tryptophan to an energy acceptor on Gln41, the experiments with ANP-labeled F-actin, before and after its photo-cross-linking, shed light on the relationship between cofilin binding and the changes in F-actin structure. The cross-linking of Gln41 to Cys374 by ANP blocked the cofilin-induced actin depolymerization and the change in FRET, but not the binding of cofilin, suggesting that the binding event and the conformational rearrangement are not coupled tightly. However, because of the flexibility of interprotomer contact sites on actin, this result does not preclude their partial realignment by cofilin. In fact, a partial rotation of actin domains by cofilin was detected recently in the disulfide cross-linked Q41C F-actin.[42] The uncoupling, whether complete or incomplete, between cofilin binding and changes in the filament structure may be taking place at lower pH conditions (~6.5), at which little, if any, depolymerization is observed. It is possible, on the basis of structural studies on human cofilin and actin at pH 6.5 and 7.7,[14] that there are two different, pH-dependent modes of cofilin binding to F-actin. Clearly, it will be interesting now to explore this possibility and to test the effect of pH on cofilin-induced changes in longitudinal contacts in F-actin using the tools described in this study.

Materials and Methods

Reagents

5-[[((2-Iodoacetyl)amino)ethyl]amino]naphthalene-1-sulfonic acid (IAEDANS), pyrene maleimide, and DED were from Molecular Probes (Eugene, OR). The ANP was a generous gift from Dr G. Hegyi (Budapest, Hungary).

Proteins

Skeletal muscle α-actin was isolated from rabbit back muscle as described.[44] The creation of yeast strains producing the Q41C, Q41C/C374S and D51C/C374S mutant actins has been described.[35,37] Dr K. Seguro (Ajinomoto Co, Kawasaki, Japan) generously provided the Ca^{2+}-independent bacterial transglutaminase. Mutant actins were purified from yeast cells by affinity chromatography on a DNase I column according to Cook *et al*.[45] To avoid contamination of yeast actin with cofilin, the DNase I column was washed with G-buffer (5.0 mM Tes (pH 7.5), 0.2 mM $CaCl_2$, 0.2 mM ATP, 1.0 mM DTT) containing 1.0 M NaCl.[46] Yeast cofilin was prepared as described[27] but with minor modifications. Briefly, WT yeast cofilin was expressed in *Escherichia coli* BL21(DE3) cells under the T7 promoter (pBAT4 plasmid).[27] Cells were grown to a density of 0.6 absorbance units, induced with 0.4 mM IPTG, harvested by centrifugation, resuspended in 20 mM Tris–HCl (pH 7.5), and lysed by sonication. The cell lysate was clarified by centrifugation, the supernatant applied to a QAE-52 column (Pharmacia Biotech) equilibrated with 20 mM Tris–HCl (pH 7.5) and the column developed with a linear 0–0.5 M NaCl gradient. Peak fractions containing cofilin were pooled, concentrated, and applied to a Sephacryl S300 gel-filtration column (Pharmacia Biotech), equilibrated with 10 mM Tris–HCl (pH 7.5), 50 mM NaCl. The peak fractions were pooled and polished by MonoQ ion-exchange chromatography using a buffer system similar to that described for the QAE-52 chromatography. The concentrations of cofilin and unlabeled skeletal muscle α-actin were determined spectrophotometrically by using the extinction coefficients $E^{1\%}_{280} = 9.2\ cm^{-1}$ and $E^{1\%}_{290} = 11.5\ cm^{-1}$, respectively. The concentrations of yeast actins and labeled skeletal muscle α-actin were measured by the Bradford protein assay[47] using native skeletal muscle α-actin as a standard.

Actin labeling

The labeling and photo-cross-linking of skeletal muscle α-actin with ANP was carried out as described.[38] Skeletal muscle α-actin was labeled with DED according to Kim *et al*.[28] Typically, ~100% ANP and ~80–90% DED-labeled actins were used in the experiments. Q41C/C374S and D51C/C374S yeast G-actin was labeled overnight, in G-buffer at 4 °C, using a threefold molar excess of IAEDANS. The degree of actin labeling was between 70% and 90%. The labeling of Q41C with pyrene maleimide was performed as described.[36] The resulting material had close to 2.0 pyrene maleimide molecules incorporated per actin. All labeled actins were purified from an excess of reagent and damaged protein by a polymerization–depolymerization cycle.

Fluorescence measurements

Fluorescence emissions spectra were recorded at 20 °C in a Spex Flurolog spectrofluorometer in G-buffer for CaATP–G-actin, and in G-buffer containing 3.0 mM $MgCl_2$ for F-actin. For direct excitation of the AEDANS, DED, and pyrene probes, the wavelengths were set at 338 nm, 334 nm and 344 nm, respectively. To monitor intrinsic tryptophan fluorescence or energy transfer from tryptophan to the above acceptor probes and to ANP, the excitation wavelength was set at 295 nm. Cofilin has a low intrinsic tryptophan fluorescence relative to that of actin (~5% of actin's fluorescence, data not shown). All tryptophan emission spectra of actin collected in the presence of cofilin were corrected for its contribution to tryptophan fluorescence. For light-scattering measurements, both the excitation and the emission wavelengths were set at 350 nm.

FRET efficiency (E) was determined by measuring the fluorescence intensity of tryptophan in the presence (F_{DA}) and in the absence (F_D) of the acceptor according to:

$$E = [1 - (F_{DA}/F_D)]/\alpha \quad (1)$$

where α is the degree of actin labeling with the acceptor.

Stopped-flow measurements

These measurements were carried out with the stopped-flow apparatus of Applied Photophysics SX·18MV (Leatherhead, UK) supplied with both the excitation and emission monochromators. For tryptophan fluorescence, the excitation and emission wavelengths were set at 290 nm and 329 nm, respectively. For light-scattering measurements, both monochromators were set at 380 nm. All stopped-flow measurements were carried out in 25 mM KCl, 2.0 mM $MgCl_2$ and 25 mM Mops (pH 7.4) at 20 °C. The temperature was controlled by water from a refrigerating bath circulating around the drive syringes and the observation chamber. For each experiment, the data were averaged over four to six consecutive pushes of stopped-flow. The data were fit with a non-linear least-squares procedure to either a single or a double-exponential expression, from which the rate constants were calculated.

Cofilin binding to actin

The equilibrium dissociation constant (K_d) for cofilin and actin was determined by fitting the changes in the fluorescence of F-actin, with the addition of cofilin, to equation (2), which assumes a stoichiometric binding of these proteins to each other:

$$\Delta F = 0.5\Delta F_{max} A^{-1}[(A + C + K_d) - \{(A + C + K_d)^2 - 4AC\}^{0.5}] \quad (2)$$

where ΔF is a fluorescence change, ΔF_{max} is the maximum fluorescence change (at a complete saturation of actin with cofilin), and A and C are the concentrations of actin and cofilin, respectively.

In the case of Q41C F-actin labeled with two pyrene maleimide molecules, the changes in the excimer band fluorescence caused by cofilin binding were fitted to equation (3), which can be used to describe cooperative processes:

$$\Delta F = \Delta F_{max} C^n/(C^n + K^n_{0.5}) \quad (3)$$

where ΔF is a fluorescence change, ΔF_{max} is the

maximum fluorescence change (at a complete saturation of actin with cofilin), C is the concentration of cofilin, n is the Hill coefficient, and $K_{0.5}$ is the concentration of cofilin at which $\Delta F = 0.5\Delta F_{max}$.

Disulfide cross-linking of QC F-actin

Immediately prior to using Q41C G-actin, DTT was removed from it on spin columns of Sephadex G-50 equilibrated with G-buffer adjusted to pH 7.4 and free of DTT. The Q41C actin recovered after two passages on spin columns was polymerized for 15 minutes, at room temperature, with 3.0 mM $MgCl_2$. The F-actin (at a concentration between 10 μM and 12 μM) was then split into two parts, for disulfide cross-linking in the absence and in the presence of equimolar amounts of cofilin. The oxidation reaction was either spontaneous or was catalyzed by 5 μM $CuSO_4$. Aliquots of the reactions were withdrawn from the mixtures at selected time-points, and the free cysteine residues on actin were blocked with 2 mM *N*-ethyl maleimide. The progress of disulfide cross-linking of Q41C F-actin was monitored by SDS-PAGE (under non-reducing conditions) by measuring the decay of the monomer actin band as a function of reaction time (using Sigmagel). The disappearance of the monomer band due to disulfide cross-linking of F-actin followed a first-order process and yielded the rate constants for actin cross-linking.

Acknowledgements

This work was supported by grants from the USPHS (AR-22031) and NSF (MCB 9904599) to E.R., a grant from the Israel Science Foundation (230/99) to A.M. and a grant from NIH (GM53807) to S.C.A.

References

1. Iida, K., Moriyama, K., Matsumoto, S., Kawasaki, H., Nishida, E. & Yahara, I. (1993). Isolation of a yeast essential gene, COF1, that encodes a homologue of mammalian cofilin, a low-M_r actin-binding and depolymerizing protein. *Gene*, **124**, 115–120.
2. Chen, J., Godt, D., Gunsalus, K., Kiss, I., Godberg, M. & Laski, F. A. (2001). Cofilin/ADF is required for cell motility during *Drosophila* ovary development and oogenesis. *Nature Cell Biol.* **3**, 204–209.
3. Carlier, M.-F., Ressad, F. & Pantaloni, D. (1999). Control of actin dynamics in cell motility. Role of ADF/cofilin. *J. Biol. Chem.* **48**, 33827–33830.
4. Bamburg, J. R. (1999). Proteins of the ADF/cofilin family: essential regulators of actin dynamics. *Annu. Rev. Cell Dev. Biol.* **15**, 185–230.
5. Bowman, G. D., Nodelman, I. M., Hong, Y., Chua, N.-H., Lindberg, U. & Schutt, C. E. (2000). A comparative structural analysis of the ADF/cofilin family. *Proteins: Struct. Funct. Genet.* **41**, 374–384.
6. Hawkins, M., Pope, B., Maciver, S. K. & Weeds, A. G. (1993). Human actin depolymerizing factor mediates a pH-sensititve destruction of actin filaments. *Biochemistry*, **32**, 9985–9993.
7. Moriyama, K. & Yahara, I. (1999). Two activities of cofilin, severing and accelerating directional depolymerization of actin filaments, are affected differentially by mutations around the actin-binding helix. *EMBO J.* **18**, 6752–6761.
8. Blanchoin, L. & Pollard, T. D. (1999). Mechanism of interaction of *Acanthamoeba* actophorin (ADF/Cofilin) with actin filaments. *J. Biol. Chem.* **274**, 15538–15546.
9. Carlier, M.-F., Laurent, V., Santolini, J., Melki, R., Didry, D., Xia, G.-X. *et al.* (1997). Actin depolymerizing factor (ADF/cofilin) enhances the rate of filament turnover: implication in actin-based motility. *J. Cell Biol.* **136**, 1307–1323.
10. Ressad, F., Didry, D., Xia, G.-X., Chua, N.-H., Pantaloni, D. & Carlier, M.-F. (1998). Kinetic analysis of the interaction of actin-depolymerizing factor (ADF)/cofilin with G- and F-actins. *J. Biol. Chem.* **273**, 20894–20902.
11. Theriot, J. A. (1997). Accelerating on a treadmill: ADF/cofilin promotes rapid actin filament turnover in the dynamic cytoskeleton. *J. Cell Biol.* **136**, 1165–1168.
12. Yeoh, S., Pope, B., Mannherz, H. G. & Weeds, A. (2002). Determining the differences in actin binding by human ADF and cofilin. *J. Mol. Biol.* **315**, 911–925.
13. McGough, A., Pope, B., Chiu, W. & Weeds, A. (1997). Cofilin changes the twist of F-actin: implications for actin filament dynamics and cellular function. *J. Cell Biol.* **138**, 771–781.
14. Galkin, V. E., Orlova, A., Lukoyanova, N., Wriggers, W. & Egelman, E. H. (2001). Actin depolymerizing factor stabilizes an existing state of F-actin and changes the tilt of F-actin subunits. *J. Cell Biol.* **153**, 75–86.
15. Holmes, K. C., Popp, D., Gebhard, W. & Kabsch, W. (1990). Atomic model of the actin filament. *Nature*, **347**, 44–49.
16. Lorenz, M., Popp, D. & Holmes, K. C. (1993). Refinement of the F-actin model against X-ray fiber diffraction data by used of a direct mutation algorithm. *J. Mol. Biol.* **234**, 826–836.
17. Owen, C. & DeRosier, D. (1993). A 13 Å map of the actin–scruin filament from the limulus acrosomal process. *J. Cell Biol.* **123**, 337–344.
18. Orlova, A. & Egelman, E. H. (1993). A conformational change in the actin subunit can change the flexibility of the actin filament. *J. Mol. Biol.* **232**, 334–341.
19. Muhlrad, A., Cheung, P., Phan, B. C., Miller, C. & Reisler, E. (1994). Dynamic properties of actin structural changes induced by beryllium fluoride. *J. Biol. Chem.* **269**, 11852–11858.
20. Strzelecka-Golaszewska, H., Mossakowska, M., Wozniak, A., Moraczewska, J. & Nakayama, H. (1995). Long-range conformational effects of proteolytic removal of the last three residues of actin. *Biochem. J.* **307**, 527–534.
21. Kim, E., Miller, C. J., Motoki, M., Seguro, K., Muhlrad, A. & Reisler, E. (1996). Myosin-induced changes in F-actin—fluorescence probing of subdomain 2 by dansyl ethylenediamine attached to Gln41. *Biophys. J.* **70**, 1439–1446.
22. Khaitlina, S. Y. & Strzelecka-Golaszewska, H. (2002). Role of the DNase-I-binding loop in dynamic properties of actin filament. *Biophys. J.* **82**, 321–334.
23. Strzelecka-Golaszewska, H., Moraczewska, J., Khaitlina, S. Y. & Mossakowska, M. (1993). Localization of the tigthly bound divalent-cation-dependent and nucleotide-dependent conformation changes in G-actin using limited proteolytic digestion. *Eur. J. Biochem.* **211**, 731–742.

24. Khaitlina, S. Y., Moraczewska, J. & Strzelecka-Golaszewska, H. (1993). The actin/actin interactions involving the N terminus of the DNase-I-binding loop are crucial for stabilization of the actin filament. *Eur. J. Biochem.* **218**, 911–920.
25. Crosbie, R. H., Miller, C., Cheung, P., Goodnight, T., Muhlrad, A. & Reisler, E. (1994). Structural connectivity in actin: effect of C-terminal modifications on the properties of actin. *Biophys. J.* **67**, 1957–1964.
26. Lappalainen, P., Fedorov, E. V., Fedorov, A. A., Almo, S. C. & Drubin, D. G. (1997). Essential function and actin binding surfaces of yeast cofilin revealed by systematic mutagenesis. *EMBO J.* **16**, 5520–5530.
27. Ojala, P. J., Paavilainen, V. & Lappalainen, P. (2001). Identification of yeast cofilin residues specific for actin monomer and PIP2 binding. *Biochemistry*, **40**, 15562–15569.
28. Kim, E., Motoki, M., Seguro, K., Muhlrad, A. & Reisler, E. (1995). Conformational changes in subdomain 2 of G-actin: fluorescence probing by dansyl ethylenediamine attached to Gln-41. *Biophys. J.* **69**, 2024–2032.
29. Takashi, R. (1988). A novel actin label: a fluorescent probe at glutamine-41 and its consequences. *Biochemistry*, **27**, 938–943.
30. Dedova, I. V., Dedov, N. V., Nosworthy, N. J., Hambly, B. D. & dos Remedios, C. G. (2002). Cofilin and DNase I affect the conformation of the small domain of actin. *Biophys. J.* **82**, 3134–3143.
31. Doyle, T., Hansen, J. E. & Reisler, E. (2001). Tryptophan fluorescence of yeast actin resolved via conserved mutations. *Biophys. J.* **80**, 427–434.
32. Kuznetsova, I. M., Yakusheva, T. A. & Turoverov, K. K. (1999). Contribution of separate tryptophan residues to intrinsic fluorescence of actin. Analysis of 3D structure. *FEBS Letters*, **452**, 205–210.
33. Lakowicz, J. R. (1999). *Principles of Fluorescence Spectroscopy*, 2nd edit., Kluwer Academic/Plenum Publishers, New York.
34. Wu, P. & Brand, L. (1994). Resonance energy transfer: methods and applications. *Anal. Biochem.* **218**, 1–13.
35. Kim, E., Wriggers, W., Phillips, M., Kokabi, K., Rubenstein, P. A. & Reisler, E. (2000). Cross-linking constraints on F-actin structure. *J. Mol. Biol.* **299**, 421–429.
36. Kim, E. & Reisler, E. (2000). Intermolecular dynamics and function in actin filaments. *Biophys. Chem.* **86**, 191–201.
37. Gerson, J. H., Kim, E., Muhlrad, A. & Reisler, E. (2001). Tropomyosin–troponin regulation of actin does not involve subdomain 2 motions. *J. Biol. Chem.* **276**, 18442–18449.
38. Hegyi, G., Mak, M., Kim, E., Elzinga, M., Muhlrad, A. & Reisler, E. (1998). Intrastrand cross-linked actin between Gln-41 and Cys-374. I. Mapping of sites cross-linked in F-actin by *N*-(4-azido-2-nitrophenyl) putrescine. *Biochemistry*, **37**, 17784–17792.
39. Pope, B. J., Gonsior, S. M., Yeoh, S., McGough, A. & Weeds, A. G. (2000). Uncoupling actin filament fragmentation by cofilin from increased subunit turnover. *J. Mol. Biol.* **298**, 649–661.
40. McGough, A. & Chiu, W. (1999). ADF/cofilin weakens lateral contacts in the actin filament. *J. Mol. Biol.* **291**, 513–519.
41. Galkin, V. E., VanLoock, M. S., Orlova, A. & Egelman, E. H. (2002). A new internal mode in F-actin helps explain the remarkable evolutionary conservation of actin's sequence and structure. *Curr. Biol.* **12**, 570–575.
42. Orlova, A., Galkin, V. E., VanLoock, M. S., Kim, E., Shvetsov, A., Reisler, E. & Egelman, E. H. (2001). Probing the structure of F-actin: cross-links constrain atomic models and modify actin dynamics. *J. Mol. Biol.* **312**, 95–106.
43. Lehrer, S. S. (1995). Pyrene excimer change as a probe of protein conformational change. *Subcell. Biochem.* **24**, 115–139.
44. Spudich, J. A. & Watt, S. (1971). Regulation of skeletal muscle contraction. I. Biochemical studies of the interaction of the tropomyosin–troponin complex with actin and the proteolytic fragments of myosin. *J. Biol. Chem.* **246**, 4866–4876.
45. Cook, R. K., Root, D., Miller, C., Reisler, E. & Rubenstein, P. A. (1993). Enhanced stimulation of myosin subfragment-1 ATPase activity by addition of negatively charged residues to the yeast actin NH_2-terminus. *J. Biol. Chem.* **268**, 2410–2415.
46. Du, J. & Frieden, C. (1998). Kinetic studies on the effect of yeast cofilin on yeast actin polymerization. *Biochemistry*, **37**, 13276–13284.
47. Bradford, M. M. (1976). A rapid and sensitive method for the quantitation of microgram quantities of protein utilizing the principle of protein–dye binding. *Anal. Biochem.* **72**, 248–254.

Edited by M. Moody

(Received 10 May 2002; received in revised form 2 September 2002; accepted 16 September 2002)